Planta (2023) 257:90
https://doi.org/10.1007/s00425-023-04125-z

ORIGINAL ARTICLE

Identification and functional characterization of three cytochrome P450 genes for the abietane diterpenoid biosynthesis in *Isodon lophanthoides*

Zuying Du[1] · Ziqiu Peng[1] · Hui Yang[1] · Haisheng Wu[1] · Jie Sun[2] · Lili Huang[1]

Received: 29 November 2022 / Accepted: 22 March 2023 / Published online: 29 March 2023

Abstract

Main conclusion **We identify two ferruginol synthases and a 11-hydroxyferruginol synthase from a traditional Chinese medicinal herb *Isodon lophanthoides* and propose their involvement in two independent abietane diterpenoids biosynthetic pathways.**

Abstract *Isodon lophanthoides* is a traditional Chinese medicinal herb rich in highly oxidized abietane-type diterpenoids. These compounds exhibit a wide range of pharmaceutical activities, yet the biosynthesis is barely known. Here, we describe the screening and functional characterization of P450s that oxidize the abietane skeleton abietatriene. We mainly focused on CYP76 family and identified 12 CYP76AHs by mining the RNA-seq data of *I. lophanthoides*. Among the 12 CYP76AHs, 6 exhibited similar transcriptional expression features as upstream diterpene synthases, including root or leaf-preferential expression pattern and highly MeJA inducibility. These six P450s were considered as first-tier candidates and functionally characterized in yeast and plant cells. In yeast assays showed that both CYP76AH42 and CYP76AH43 were ferruginol synthases hydroxylating the C12 position of abietatriene, whereas CYP76AH46 was characterized as a 11-hydroxyferruginol synthase which catalyzes two successive oxidations at C12 and C11 of abietatriene. Heterologous expression of three CYP76AHs in *Nicotiana benthamiana* resulted in the formation of ferruginol. qPCR analysis showed *CYP76AH42* and *CYP76AH43* were mainly expressed in the root, which was consistent with the distribution of ferruginol in the root periderms. *CYP76AH46* was primarily expressed in the leaves where barely ferruginol or 11-hydroxyferruginol was detected. In addition to distinct organ-specific expression pattern, three CYP76AHs exhibited different genomic structures (w or w/o introns), low protein sequence identities (51–63%) and were placed in separate subclades in the phylogenetic tree. These results suggest that the identified CYP76AHs may be involved in at least two independent abietane biosynthetic pathways in the aerial and underground parts of *I. lophanthoides*.

Keywords *Isodon lophanthoides* · Cytochrome P450 · Ferruginol synthase · Methyl jasmonate · Secondary metabolism

Abbreviations

diTPS	Diterpene synthase
(+)-CPS	(+)-Copalyl diphosphate synthase
P450	Cytochrome P450
MeJA	Methyl jasmonate
GC–MS	Gas chromatography–mass spectrometry
GGPP	Geranylgeranyl diphosphate
GGOH	Geranylgeraniol
TIC	Total ion chromatogram

Communicated by Anastasios Melis.

✉ Lili Huang
lilihuang@gzucm.edu.cn

[1] Institute of Medicinal Plant Physiology and Ecology, School of Pharmaceutical Science, Guangzhou University of Chinese Medicine, Guangzhou 510006, China

[2] Key Laboratory of Bioorganic Synthesis of Zhejiang Province, College of Biotechnology and Bioengineering, Zhejiang University of Technology, Hangzhou, Zhejiang, China

Introduction

Isodon lophanthoides var. gerardiana is a traditional Chinese medicinal herb with a wide range of activities including anti-hepatitis, anti-jaundice and anti-microbial (Fig. 1a) (Lin et al. 2011). Highly oxidized abietane-type diterpenoids are the main bioactive constituents in *I. lophanthoides* (Sun et al. 2006; Liu et al. 2017). Among them royleanone-type diterpene quinones decorated with a hydroxy-*para*-quinone moiety in the ring C is one of the most abundant abietanes (Fig. 1b) (Yang et al. 2011; Ladeiras et al. 2016 ; Lin et al. 2016). Besides the quinonoid C ring, the abietane quinones in *I. lophanthoides* also have hydroxyl or carbonyl functionalities on C-7, C-15 and C-17 (Fig. 1b). To date, most studies on *I. lophanthoides* have focused on its phytochemistry and pharmacology. However, the biosynthesis of these compounds in the native plant is poorly learned.

Plant diterpenoid biosynthesis is initiated with diTPS which catalyzes the first committed step to form the diterpene scaffold (Chen et al. 2011). Our previous work revealed three diTPSs, including two (+)-copalyl diphosphate synthases ((+)-CPSs) and one miltiradiene synthase, which catalyze the formation of abietane carbon skeleton miltiradiene in *I. lophanthoides* (Yang et al. 2021). Next, various modifying enzymes decorate the diterpene scaffold and among them oxidation typically comes first to provide anchoring points for multiple transferases (e.g., methyltransferases, glycosyltransferases and acyltransferases) (Zi et al. 2014; Mafu et al. 2017). In plants, most of the terpene oxidation reactions are catalyzed by P450s, while some can be carried out by dioxygenases or dehydrogenases (Bathe and Tissier 2019a; Hansen et al. 2021). To date, a limited number of CYP families have been reported to be involved in specialized diterpene metabolism represented by CYP725 in taxane biosynthesis (Xiong et al. 2021), CYP720B in conifer diterpene resin acid biosynthesis (Ro et al. 2005; Hamberger et al. 2011), CYP714 in steviol glycoside biosynthesis (Brandle and Telmer. 2007; Ceunen and Geuns. 2013) and CYP76 in labdane-related diterpenoid biosynthesis (Bathe et al. 2019b).

Among them CYP76 is a major contributor in the oxidation of diterpenoids in the Lamiaceae. One of the most well-studied subfamilies is CYP76AH, which includes ferruginol synthase and 11-hydroxyferruginol synthase. The abietane skeleton miltiradiene undergoes spontaneous oxidation to form abietatriene. Ferruginol synthase then catalyzes a single oxidative reaction at C12 position of abietatriene to form ferruginol, whereas 11-hydroxyferruginol synthase catalyzes two successive oxidations at C12 and C11 positions of abietatriene, leading to the formation of 11-hydroxyferruginol. These enzymes have been identified in *Salvia miltiorrhiza* ('danshen' in Chinese) (Guo et al. 2013, 2016), rosemary (*Rosmarinus officinalis*) and Greek sage (*S. fruticosa*) (Zi and Peters 2013; Božić et al. 2015). Their involvements in the biosynthesis of phenolic diterpenoid tanshinone and carnosic acid have been well elucidated (Guo et al. 2016;

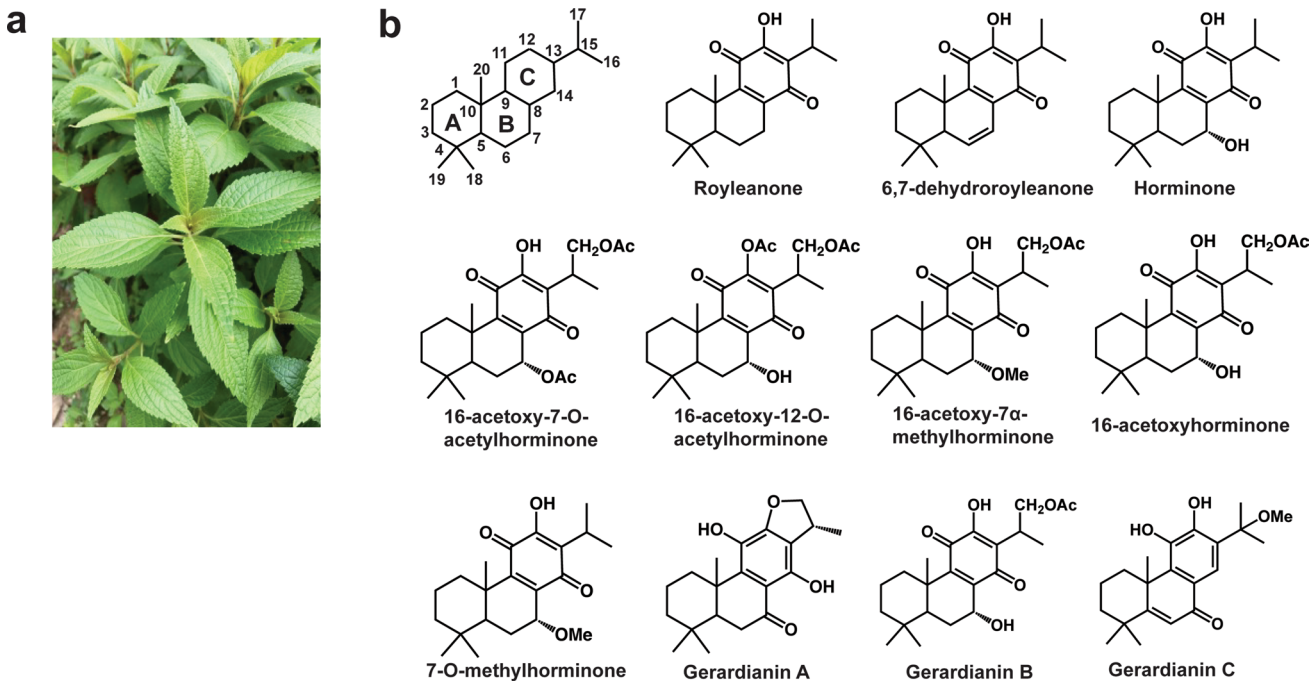

Fig. 1 **a** Image of *I. lophanthoides*; **b** structures of reported oxidized abietane-type diterpenoids in *I. lophanthoides*

Ignea et al. 2016; Scheler et al. 2016). CYP76AH members from *Coleus forskohlii* are able to catalyze five successive oxidations on manoyl oxide to form important intermediate of bioactive diterpene forskolin (Pateraki et al. 2017). A closely related subfamily CYP76AK oxidizes a variety of diterpene substrates (e.g., miltiradiene, ferruginol, and 11-hydroxyferruginol) at C20 position and was named C20 oxidases (Ignea et al. 2016; Scheler et al. 2016). CYP76AM subfamily is involved in the biosynthesis of labdane-related phytoalexins in rice (Wang et al. 2012; Wu et al. 2013). Besides CYP76 family, a few members from CYP71 (e. g. CYP71D, CYP71Z and CYP71BE), CYP82 and CYP728 are reported to oxidize the labdane-related diterpenoids (Wu et al. 2011; Ignea et al. 2016; Tu et al. 2020; Ma et al. 2021; Muchlinski et al. 2021; Hansen et al. 2022).

Our previous work showed distinct diterpenoid profiles in the root and leaf tissues from *I. lophanthoides*. The root contains a large amount of miltiradiene, abietatriene and ferruginol while mainly neoabietadiene with trace amounts of levopimaradiene and abietadiene were detected in the leaf (Yang et al. 2021). We also identified two (+)-CPSs with apparent root or leaf-preferential expression pattern and this attracted our interest to explore if different P450s are contributing to the biosynthesis of abietane diterpenoids in this plant. We mainly focus on CYP76 subfamily due to its predominant role in the biosynthesis of labdane-related diterpenoids. By mining previous transcriptomic data of *I. lophanthoides* roots and leaves, we identified 18 P450 candidates belonging to CYP76 subfamily. After two rounds of screenings, six CYP76AHs were considered as strong candidates. Functional characterization in yeast and plant cells demonstrates three of them are ferruginol or 11-hydroxyferruginol synthases. We further study the genomic structure and phylogeny of these three CYP76AHs and propose at least two independent abietane biosynthetic pathways represented by diTPSs and P450s in the above- and underground part of *I. lophanthoides*.

Materials and methods

Plant materials and sample preparations

For RNA-seq and tissue-specific expression pattern analysis, leaf and root samples were collected from the Yaowang Mountain in Guangzhou University of Chinese Medicine (113° E, 23° N). For MeJA treatment, *I. lophanthoides* seeds were collected form Yaowang Mountain and sterilized with 70% ethanol for 1 min followed by 10% sodium hypochlorite (NaOCl) for 10 min. The sterile seeds were germinated on Murashige and Skoog (MS) media supplemented with 3% sugar and 0.7% agar and grown in a growth chamber with a 12/12-h light/dark photoperiod at 24 °C. 40-day-old *I. lophanthoides* seedlings were sprayed with 100 µM MeJA (Sigma-Aldrich) (first dissolved in ethanol to make a 100 mM stock and then diluted to 100 µM with distilled water) and the ethanol solution was used as a mock. Leaf samples were harvested at 0 h, 6 h, 12 h, 24 h and 48 h after treatment and each time point included three independent biological replicates. For each replicate, 50 mg of young leaves from the apical top of a single *I. lophanthoides* seedling was collected, immediately chilled in liquid nitrogen and stored at − 80 °C until use for total RNA extraction. For plant transient expression, *N. benthamiana* seeds were germinated in soil and grown in a greenhouse with a 16/8-h light/dark photoperiod at 25 °C.

Quantitative real-time PCR (qRT-PCR)

Total RNAs were extracted using SteadyPure Plant RNA Extraction Kit (Accurate biotechnology) following the manufacturer's recommendations. Total RNAs were reverse transcribed using the *Evo M-MLV* RT kit with gDNA clean for qPCR (Accurate biotechnology). qRT-PCR reactions were performed with SYRB Green *Pro Taq* HS qPCR premix (Accurate biotechnology) on a Bio-Rad CFX96 Real-time instrument using the two-step cycling parameters: 95 ℃ for 30 s, followed by 40 cycles of 95 ℃ for 5 s, 60 ℃ for 30 s. Melt curve analysis was performed by increasing the temperature from 65 to 95 ℃ in 0.5 ℃ increments. Relative transcript abundance was evaluated using ΔC_T and $\Delta\Delta C_T$ method based on an *I. lophanthoides actin* as reference gene. The fold change was presented as the mean ± SEM of three biological replications, with each replication performed in three technical replicates. All primers used for qRT-PCR are given in Table S2.

Cloning of full-length P450 cDNA

P450 genes were cloned from cDNA generated from root or leaf total RNA using TransScript One-step gDNA removal and cDNA Synthesis SuperMix (Trans Gen). The full-length cDNAs were amplified with Phusion High-Fidelity DNA polymerase (New England BioLabs). FL cDNAs were then ligated into the HIS pESC yeast expression vector (Agilent Technology) and verified by sequencing. All primers are given in Table S2.

Functional characterization of P450s in engineered yeast cells

Yeast strain YS101 (MATα, gal80Δ::loxP, trp1-289::PGAL1-tHMGR_PGAL10-BTS1-ERG20_TRP1, ura3-52::PGAL1-IlCPS3T87_PGAL10-IlKSL1T41_URA3, leu2-3/112, his3Δ1, MAL2-8c, SUC2) was constructed by overexpressing a truncated version of IlCPS3 and IlKSL1

based on strain YS100 (Yang et al. 2021). Specifically, the upstream and downstream homologous arms were cloned from strain BY4741 with the primers ura3-Up-F/tADH1-ura3-Up-R and URA3-ura3-Down-F/ura3-Down-R, respectively. URA3 was cloned from the pESC-URA vector with the primers tCYC1-pURA3-F/ura3-tURA3-R. The DNA fragment of PGAL1-IlCPS3T87_PGAL10-IlKSL1T41 was cloned from the construct pESC-URA::IlCPS3T87/IlKSL1T41 with the primers ura3-tADH1-F/pURA3-tCYC1-R. The DNA fragments above were integrated into the genome of YS100 as previously described (Yang et al. 2021). All primers used are listed in Table S2.

Plasmids encoding P450s were transformed into the yeast strain YS101 in combination with IlCPR1 by lithium acetate method (Gietz and Woods 2002). A 11-hydroxyferruginol synthase from *R. officinalis* (*RoCYP76AH22*, Scheler et al. 2016) was used as reference gene. The diterpene products were collected by two-phase flask cultivation as previously described (Yang et al. 2021).

Transient expression of P450s in *Nicotiana benthamiana*

CYP76AH42, *CYP76AH43* and *CYP76AH46* were transiently co-expressed in *N. benthamiana* with two diTPS (*IlCPS3* and *IlKSL1*) and a P450 reductase gene (*IlCPR1*) from *I. lophanthoides*. Full-length cDNAs of these six genes were cloned into the pEAQ-HT expression vector (Sainsbury et al. 2009) and transformed into *Agrobacterium tumefaciens* LBA4404-competent cells. Each of the *Agrobacterium* cultures were collected, washed and diluted to an optical density at 600 nm of 0.8 with *Agrobacterium* induction buffer (10 mM MES, pH 5.6, 10 mM $MgCl_2$, 100 µM acetosyringone). Different combinations prepared from equal volumes of each *Agrobacterium* cultures were infiltrated into the abaxial side of 6-week-old *N. benthamiana* leaves with a needleless 1-ml syringe. 100 mg leaf samples were harvested 5 days after infiltration, exacted with 3 ml hexane and analyzed by GC–MS.

GC–MS analysis

GC–MS analyses were performed in an Agilent 8890 GC machine (Agilent) equipped with an HP-5MS column (0.25 mm ID × 30 m, 0.25 µm film thickness, Agilent) and an Agilent 5977B mass selective detector with electron ionization (EI) source. One microliter of sample was injected into a splitless injection mode and the carrier gas was helium with a flow rate of 1.0 mL/min. The injection temperature was 250 ℃. The GC oven temperature was set at 50 ℃ for 2 min, followed by a 20 ℃/min ramp to 200 ℃, and then followed with a linear ramp at a rate of 5 ℃/min to 280 ℃, held at 280 ℃ for 5 min. An alternative GC program is starting at 50 ℃ for 2 min, followed by an 8 °C/min ramp to 280 ℃, held at 280 ℃ for 5 min. Full mass spectra were generated for metabolite identification by scanning within the m/z range of 40–550. The identity of the resulting diterpenoid was determined by comparison of product profiles with those of previously characterized plant P450s.

Phylogenetic analysis

Phylogenetic analysis was conducted from ClustalW alignments by the Neighbor-joining method using MEGA version 11, based on the JTT substitution model (Tamura et al. 2021). The bootstrap consensus tree was inferred from 1000 replicates. A *Solanum melongena* CYP76A1 are used as outgroup. The abbreviations and accession numbers of protein sequences used are given in Table S3.

Statistical analysis

All experiments were repeated using at least three biological replicates. Data were presented as mean ± SEM. The relative transcript abundance of *diTPSs* and *CYP76AHs* in the control or MeJA-treated groups were subjected to unpaired Student's *t* test for comparison (mock versus MeJA). Statistical significance is indicated by $*P < 0.05$; $**P < 0.01$; $***P < 0.001$. The Pearson correlation coefficient (Pearson's *r*) was computed to access the similarity of transcriptional expression patterns between *diTPSs* and *CYP76AHs* after MeJA treatment.

Results

Screening of *I. lophanthoides* P450 candidates in abietane-type diterpene biosynthesis

A cDNA library was constructed using total RNA from *I. lophanthoides* roots and leaves and sequenced by Illumina Hiseq 4000 platform. After removing adapter sequences and low-quality reads, 56,103,989 high-quality clean reads were obtained and de novo assembled into 46,787 unigenes (Yang et al. 2021). To identify the *P450* genes involved in abietane-type diterpene biosynthesis in *I. lophanthoides*, we mainly focused on CYP76 family and identified 18 CYP76 genes by homology searches. Among them, 12 belong to the CYP76AH subfamily, indicating a high presence of CYP76AH transcripts in *I. lophanthoides*. The 12 CYP76AHs were named as CYP76AH42-51 by the P450 Nomenclature Committee (Table S1).qPCR analysis showed 9 out of 12 *CYP76AH*s exhibit leaf- or root-preferential expression pattern, except for *CYP76AH49* which was expressed in both tissues and *CYP76AH47* and *CYP76AH48* which were barely expressed in neither tissue (Fig. 2a).

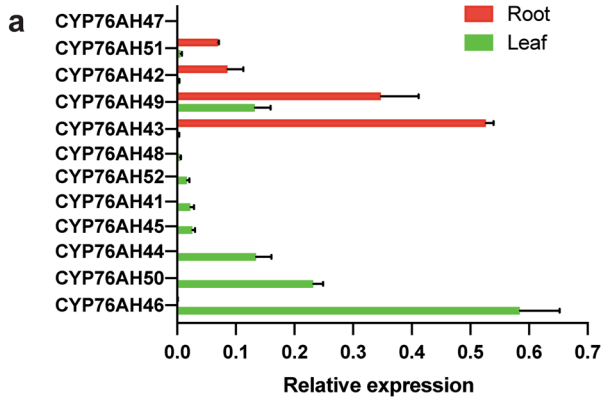

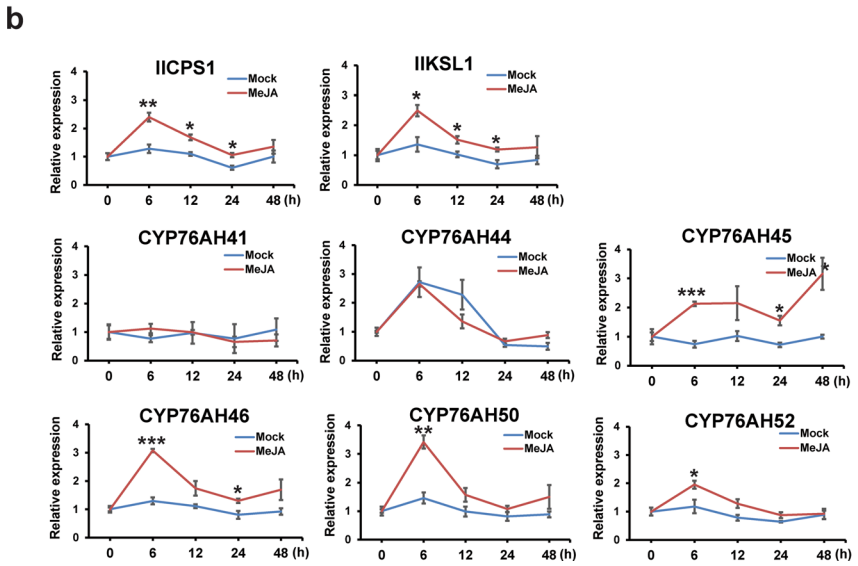

c

Gene	Pearson's r	
	IICPS1	IIKSL1
IICPS1	1.00	0.96
IIKSL1	0.96	1.00
CYP76AH41	0.42	0.26
CYP76AH44	0.87	0.81
CYP76AH45	0.37	0.24
CYP76AH46	0.95	0.95
CYP76AH50	0.95	0.95
CYP76AH52	0.92	0.94

Fig. 2 Transcriptional gene expression of candidate *P450s* in *I. lophanthoides* seedlings. **a** qRT-PCR analysis of relative transcript levels of *P450* candidates in roots and leaves; **b** qRT-PCR analysis of relative transcript levels of *diTPSs* and *P450s* after 100 μM MeJA treatment. The transcript abundance was normalized to the internal reference *actin* gene. Data were presented as mean ± SEM based on triplicate measurements of three biological replicates. Statistically significant differences between the mock and MeJA-treated groups were calculated by Student's *t* test and statistical significance is indicated by $*P<0.05$; $**P<0.01$; $***P<0.001$; **c** Pearson correlation analysis of transcriptional expression patterns between *diTPSs* and *CYP76AHs* after MeJA treatment. *IlCPS1* and *IlKSL1* were used as queries, respectively. Pearson's *r* values greater than 0.8 were highlighted in red

Specifically, among the nine *CYP76AHs*, three were mainly expressed in the root and six were mainly expressed in the leaves. Highest relative transcript abundance was detected with *CYP76AH43* in roots and *CYP76AH46* in leaves (Fig. 2a). This tissue-specific transcriptional expression pattern of *CYP76AHs* is similar as upstream (+)-CPSs, which contains a leaf-preferential *IlCPS1* and a root-preferential *IlCPS3* (Yang et al. 2021).

Considering both of the leaf-preferential diTPS genes *IlCPS1* and *IlKSL1* are highly inducible by MeJA (Yang et al. 2021), we treated the plants with 100 μM MeJA and measured the transcript levels of six leaf-preferential *CYP76AHs* by qPCR. We found four *CYP76AHs* (*CYP76AH44, CYP76AH46*, *CYP76AH50* and *CYP76AH52*) were induced by MeJA and the highest transcript abundance reached at 6 h after MeJA treatment which was exactly same as *IlCPS1* and *IlKSL1* (Fig. 2b). Further, Pearson correlation analysis demonstrated a strong correlation of transcriptional expression patterns between these four *CYP76AHs* and both *IlCPS1* and *IlKSL1* after MeJA treatment (Pearson's $r>0.80$) (Fig. 2c). Notably, expression of *CYP76AH44* in both mock and MeJA-treated groups were induced and reached highest level at 6 h, indicating it may be stress-responsive. For *CYP76AH52*, although it was significantly induced by MeJA, its native expression level was much lower than other *CYP76AHs*, making it a weak candidate. In conclusion, after two rounds of screening, six *CYP76AHs* including three leaf-preferential *CYP76AHs* (*CYP76AH44, CYP76AH46* and *CYP76AH50*) and three root-preferential *CYP76AHs* (*CYP76AH42*, *CYP76AH43* and *CYP76AH51*)

were considered as first-tier candidates for abietane-type diterpenoids biosynthesis in *I. lophanthoides*. The remaining six CYP76AHs were not completely excluded but considered as second-tier candidates.

In yeast functional characterization of *I. lophanthoides CYP76AHs*

Functional characterization of *I. lophanthoides* CYP76AHs was carried out by heterologous expression in *Saccharomyces cerevisiae*. Each CYP76AH was combined with an *I. lophanthoides* cytochrome P450 reductase (IlCPR1) and transformed into an engineered yeast strain YS101 which overexpressing yeast 3-hydroxy-3-methylglutaryl-CoA reductase (truncated version, *tHMGR*), farnesyl diphosphate synthetase (*ERG20*), geranylgeranyl diphosphate synthase (*BTS1*) and *I. lophanthoides IlCPS3* and *IlKSL1* to allow for sufficient supply of precursor miltiradiene. After growth in flasks for 120 h (Peng et al. 2017), the diterpene products were extracted and analyzed using GC–MS.

P450 activity was detected for CYP76AH42, CYP76AH43 and CYP76AH46 (Fig. 3a), while no products were found for CYP76AH44, CYP76AH50 and CYP76AH51. Co-expression of IlCPR1 with either CYP76AH42 or CYP76AH43 resulted in a single peak with exactly same retention time and mass spectrum as ferruginol (Fig. 3a, peak 5). Co-expression of CYP76AH46 and IlCPR1 led to the formation of three products including ferruginol, 11-hydroxyferruginol (Fig. 3a, peak 6) and its spontaneously oxidized product abietaquinone (Fig. 3a, peak 7), as identified by comparison to the known products of a 11-hydroxyferruginol synthase from *R. officinalis* (*RoCYP76AH22*, Scheler et al. 2016). In addition, we also tested the activities of 6 second-tier CYP76AH candidates and no new product was detected.

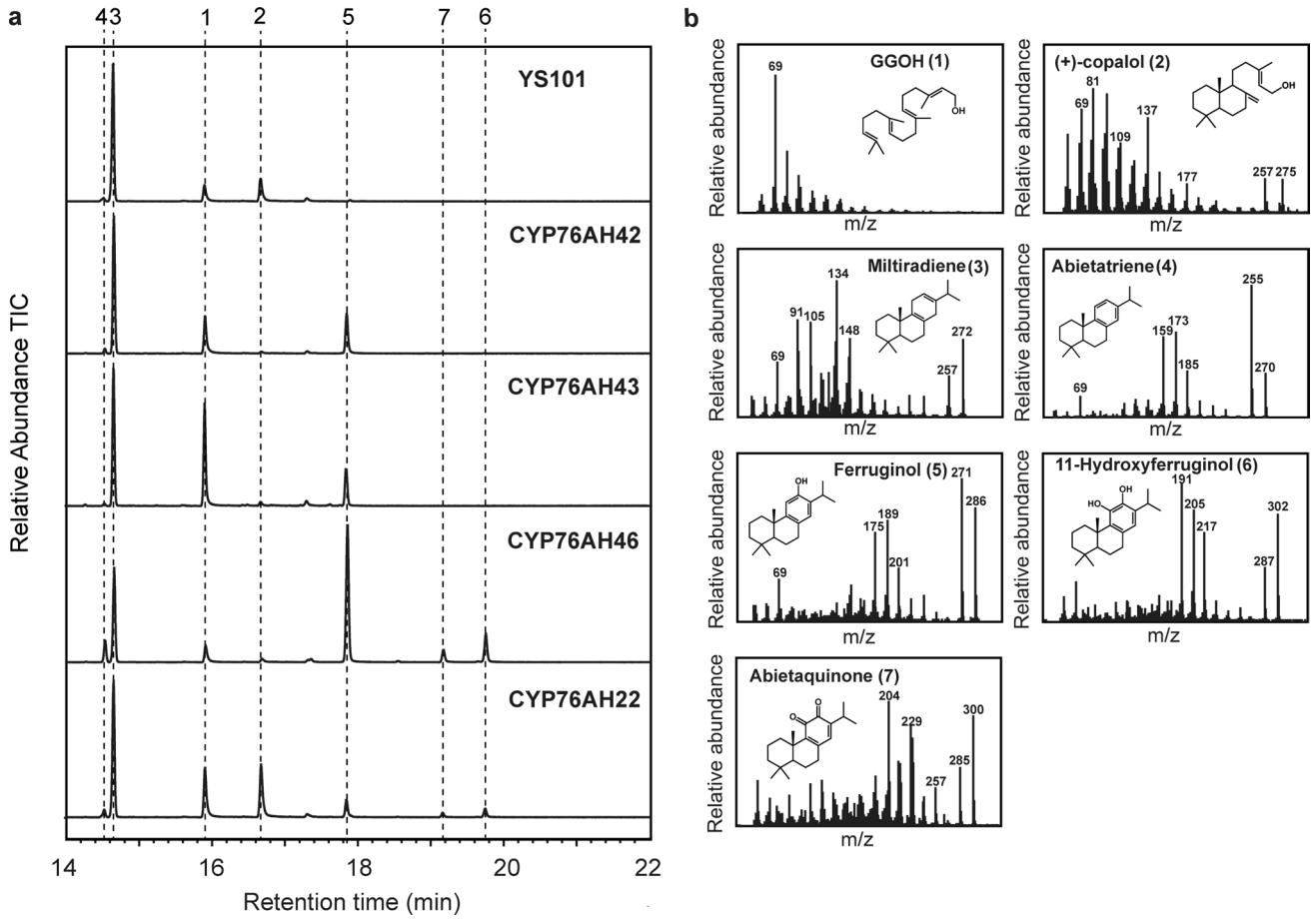

Fig. 3 Functional characterization of CYP76AH42, CYP76AH43 and CYP76AH46 in yeast cells. **a** GC/MS analysis (TIC) of extracts from the yeast strain YS101 co-expressing indicated P450 and a P450 reductase from *I. lophanthoides* (IlCPR1). A CYP76AH22 from *R. officinalis* was used as reference gene. The labeled peaks correspond to GGOH (1, dephosphorylated derivative of GGPP), (+)-copalol (2, dephosphorylated derivative of (+)-CPP), miltiradiene (3), abietatriene (4), ferruginol (5), 11-hydroxyferruginol (6) and abietaquinone (7); **b** mass spectra of the compounds identified in **a**

In plant functional characterization of three *I. lophanthoides* CYP76AHs

In case the P450 product profiles may not be identical in microbial and plant cells, we investigated the *in planta* activity of three CYP76AHs by Agrobacterium-mediated transient expression in *N. benthamiana* leaves. Full-length *CYP76AH42*, *CYP76AH43* and *CYP76AH46* were cloned into the pEAQ-HT expression vector and co-expressed with *IlCPS3*, *IlKSL1* and *IlCPR1*. GC–MS analysis showed extracts from *N. benthamiana* leaves overexpressing *CYP76AH42*, *CYP76AH43* and *CYP76AH46* all yielded a new peak identified as ferruginol (Fig. 4). No product of ferruginol was detected in the *N. benthamiana* leaves transiently overexpressed the empty vector pEAQ-HT or the combination of *IlCPS3*, *IlKSL1* and *IlCPR1* (Fig. S1). The amount of ferruginol detected in the plant cells was significantly lower compared to that in yeast cells. In addition, no 11-hydroxyferruginol was detected in *N. benthamiana* leaves overexpressing *CYP76AH46*.

Phylogenetic analysis of CYP76AH subfamily in *I. lophanthoides*

We aligned the protein sequences of IlCYP76AH42, IlCPY76AH43 and IlCYP76AH46 with other functionally characterized CYP76 proteins for phylogenetic analysis. The results showed the phylogeny was clearly divided into two clades representing CYP76AH and CYP76AK subfamilies (Fig. 5). Two distinct subclades are apparent for CYP76AH clade. Both IlCPY76AH42 and IlCYP76AH43 belong to the first subclade that comprise known ferruginol synthases and 11-hydroxyferruginol synthases. Specifically, CYP76AH42 is most closely clustered with a ferruginol synthase from *Isodon rubescens* (Jin et al. 2017) and three 11-oxo-13R-manoly oxide from *C. forskohlii* (Pateraki et al. 2017). These five P450s form a single branch adjacent to the branch

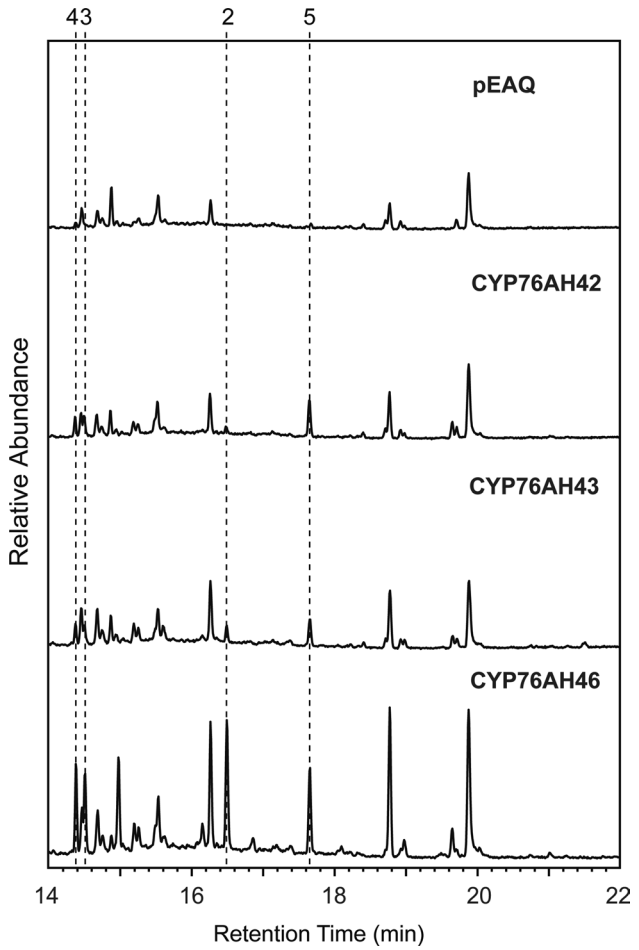

Fig. 4 Functional characterization of CYP76AH42, CYP76AH43 and CYP76AH46 in plant cells. GC/MS analysis (selected m/z signals: 255, 257, 270, 272, 286, 300 and 302) of hexane exacts from *N. benthamiana* transiently expressing CYP76AH42, CYP76AH43 and CYP76AH46 in combination with IlCPS3, IlKSL1 and IlCPR1. The labeled peaks correspond to (+)-copalol (2, dephosphorylated derivative of (+)-CPP), miltiradiene (3), abietatriene (4) and ferruginol (5)

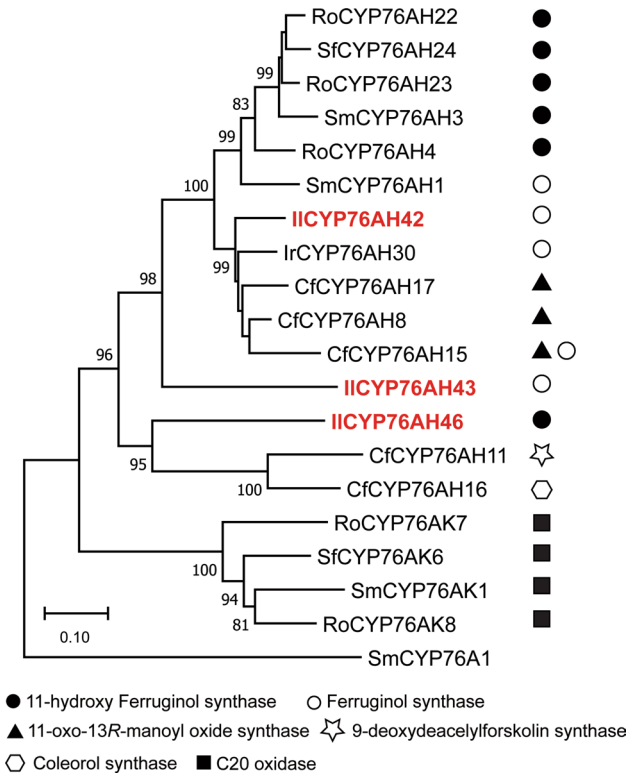

Fig. 5 Phylogeny of *I. lophanthoides* CYP76AH42, CYP76AH43 and CYP76AH46. Neighbor-joining tree of three IlCYP76AHs with known CYP76AHs based on aligned protein sequences. A *Solanum melongena* CYP76A1 are used as outgroup. Branches with bootstrap support of > 80% (1000 repetitions) are showed. The scale bar indicates 0.1 amino acid substitutions per site. Protein abbreviations and accession numbers are listed in Table S3

comprising known ferruginol/11-hydroxyferruginol synthases form rosemary, danshen and Greek sage (Guo et al. 2013; Ignea et al. 2016; Scheler et al. 2016). IlCYP76AH43 forms a separate branch adjacent to the branch containing IlCYP76AH42 (Fig. 5). Regarding CYP76AH46, despite the similar catalytic functions, it is not clustered with any known ferruginol or 11-hydroxyferruginol synthases. Instead, it is clustered with a 9-deoxydeacelylforskolin synthase and a coleorol synthase in forskolin biosynthesis (Pateraki et al. 2017). These evidences suggest CYP76AH42/43 and CYP76AH46 are likely involved in two separate abietane biosynthetic pathways in *I. lophanthoides.*

Discussion

I. lophanthoides is a traditional Chinese herb and has a long history being used for treatment of hepatitis, jaundice and cholecystitis (Lin et al. 2011; Yang et al. 2011). Modern phytochemistry and pharmacology showed oxygenated abietane-type diterpenes are the main active constituents in *I. lophanthoides*, yet the biosynthesis has not been elucidated. Here we report the screening and functional characterization of three *CYP76AHs* encoding ferruginol synthases and 11-hydroxyferruginol synthase in *I. lophanthoides*.

The biosynthesis of carbon skeleton of abietane diterpenoids in *I. lophanthoides* has been well established in our previous work (Yang et al. 2021). Three diTPSs including a leaf-preferential (+)-CPS (IlCPS1), a root-preferential (+)-CPS (IlCPS3) and a universal expressed miltiradiene synthase (IlKSL1) catalyze the formation of miltiradiene/abietatriene in *I. lophanthoides*. To explore the downstream P450 genes we mainly focus on CYP76 family which is a predominant P450 family in specialized diterpenoid metabolism. By mining the RNA-seq data of root and leaf (Yang et al. 2021), 12 CYP76AH genes were identified from 18 CYP76 genes. Interestingly, we found 9 out of 12 CYP76AH candidates exhibit apparent root- or leaf-preferential transcriptional expression pattern. This gives a clue that different P450s may be in charge of oxidation steps in different organs of *I. lophanthoides*, which is similar as upstream (+)-CPSs. We further narrowed down the six leaf-preferential candidate CYP76AHs by MeJA induction test according to the MeJA inducibility of upstream diTPSs. Finally, six organ-preferential or MeJA inducible CYP76s were considered as first-tier candidates and successfully led to the identification of two ferruginol synthases (CYP76AH42 and CYP76AH43) and one 11-hydroxyferruginol synthase (CYP76AH46).

It is worth mentioning that 11-hydroxyferruginol was only detected in the yeast cells overexpressing CYP76AH46, but not in the *N. benthamiana* leaves transiently overexpressing CYP76AH46. Previous studies have shown that endogenous modifying enzymes from *N. benthamiana* may interfere with the introduced pathway and resulted in poor yield of the target compounds. This has been demonstrated in the reconstitution of sesquiterpene and diterpene biosynthetic pathways, e.g., artemisinin (van Herpen et al. 2010; Ting et al. 2013), parthenolide (Liu et al. 2014) and carnosic acid (Bath et al. 2019a). In our study, considering the amount of ferruginol detected in the exacts from *N. benthamiana* leaves was much lower than that in the yeast cells, it is reasonable to assume most of the ferruginol synthesized in the plant cells was likely modified by tobacco endogenous enzymes (e.g., glycosyltransferase and methyltransferase) and largely restricted the formation of 11-hydroxyferruginol. Regarding the three inactive first-tier CYP76AH candidates, there is a possibility that they may involve in the downstream oxidative reactions.qRT-PCR analysis revealed *CYP76AH42* and *CYP76AH43* were mainly expressed in the roots of *I. lophanthoides*, which was consistent with the distribution of miltiradiene, abietatriene and ferruginol in the root periderms (Yang et al. 2021). In contrast, although *IlCPS1* and *CYP76AH46* were predominantly expressed in leaves, the corresponding products (e.g., miltiradiene and ferruginol) have not been detected in the aerial parts of *I. lophanthoides* (Yang et al. 2021). This suggests that these intermediates are likely further modified and transformed into more complex abietanes in the aerial parts of *I. lophanthoides*.

The involvement of ferruginol synthase and 11-hydroxyferruginol synthase in the biosynthesis of tanshinone and carnosic acid have been well elucidated. In danshen, a ferruginol synthase (CYP76AH1) and a 11-hydroxyferruginol synthases (CYP76AH3) catalyze the C12 and C7/C11/C12 oxidation of abietatriene, respectively (Bathe et al. 2019b). In rosemary, three 11-hydroxyferruginol synthases (CYP76AH4, CYP76AH22 and CYP76AH24) have been identified to catalyze the formation of important intermediate 11-hydroxyferruginol in the biosynthesis of carnosic acid (Ignea et al. 2016; Scheler et al. 2016). Scheler and coworkers (2016) have reported the mutagenesis of three amino acid residues is sufficient to convert the ferruginol synthase CYP76AH1 (D301, N303 and V479) into a 11-hydroxyferruginol synthase (E301, S303 and F478), vice versa. The three positions are conserved in the ferruginol synthases and 11-hydroxyferruginol synthases isolated from danshen, rosemary and Greek sage (Scheler et al. 2016). Interestingly, none of the three P450s identified in this study has exactly same residues in the corresponding positions. Both CYP76AH42 and CYP76AH43 have a glutamic acid at the position 301, which is identical to 11-hydroxyferruginol synthase (Fig. S2). For CYP76AH46, the corresponding residues at the three positions are E301, S303 and A478, respectively (Fig. S2). This indicated the critical amino acid residues determining the product specificity may vary in different species.

Unlike the highly identical ferruginol/11-hydroxyferruginol synthases in danshen (80%) or rosemary (88%-95%), CYP76AH42, CYP76AH43 and CYP76AH46 in *I. lophanthoides* share low protein sequence identities of 51–63% with each other (Fig. S3). Phylogeny reveals CYP76AH42/43 and CYP76AH46 are clearly located in two separate subclades within CYP76AHs. Both CYP76AH42 and CYP76AH43 belong to the first subclade which comprising known ferruginol/11-hydroxyferruginol synthases. However, CYP76AH46 is not clustered with any known 11-hydroxyferruginol synthase, instead it is clustered with a CYP76AH11 and a CYP76AH16 from *C. forskohlii* which oxidize manoyl oxide in forskolin biosynthesis (Pateraki et al. 2017). Based on the low protein sequence identity, separate phylogeny localization and distinct tissue-specific expression pattern between CYP76AH42/43 and CYP76AH46, it is reasonable to assume that independent biosynthetic ways of oxidized abietane diterpenes may exist in the above and underground part of *I. lophanthoides* (Fig. 6). The aboveground pathway is represented by IlCPS1, IlKSL1 and CYP76AH42/43, while the underground pathway is represented by IlCPS3, IlKSL1 and CYP76AH46 (Fig. 6). Different biotic and abiotic factors confronted by aerial and underground organs may be the driving forces lead to the two independent abietane diterpenes biosynthetic ways in *I. lophanthoides*. The highly inducible *diTPS* and *P450* genes in the aerial parts indicate the biosynthesis of oxidized abietane diterpenes might play an important role in plant defense under multiple stress conditions.

Although both CYP76AH42 and CYP76AH43 are root-preferential expressed ferruginol synthases and belong to the same subclade in CYP76AHs, they do not cluster together in the phylogenetic tree (Fig. 5). CYP76AH42 is most closely clustered with a ferruginol synthase from *I. rubescens* (Jin et al. 2017) and three 11-oxo-13R-manoly oxide from *C. forskohlii* (Pateraki et al. 2017). These five P450s form a single branch adjacent to the branch comprising known ferruginol/11-hydroxyferruginol synthases. CYP76AH43 form a single branch in the same subclade (Fig. 6). In addition, the genomic structure of CYP76AH43 is quine being intronless, while CYP76AH42 contains two exons and one intron which is similar as CYP76AH46 (Fig. S4). This indicates CYP76AH42 and CYP76AH43 may have evolved from a same ancestor, but experienced different intron gain and loss events. The physiological roles and evolutions of these ferruginol synthases need to be further explored in future studies.

Conclusions

Here, we characterized three phytochrome P450s belonging to the CYP76AH subfamily (CYP76AH42, 43 and 46), which oxidize the C11 or C12 position of abietane skeletons

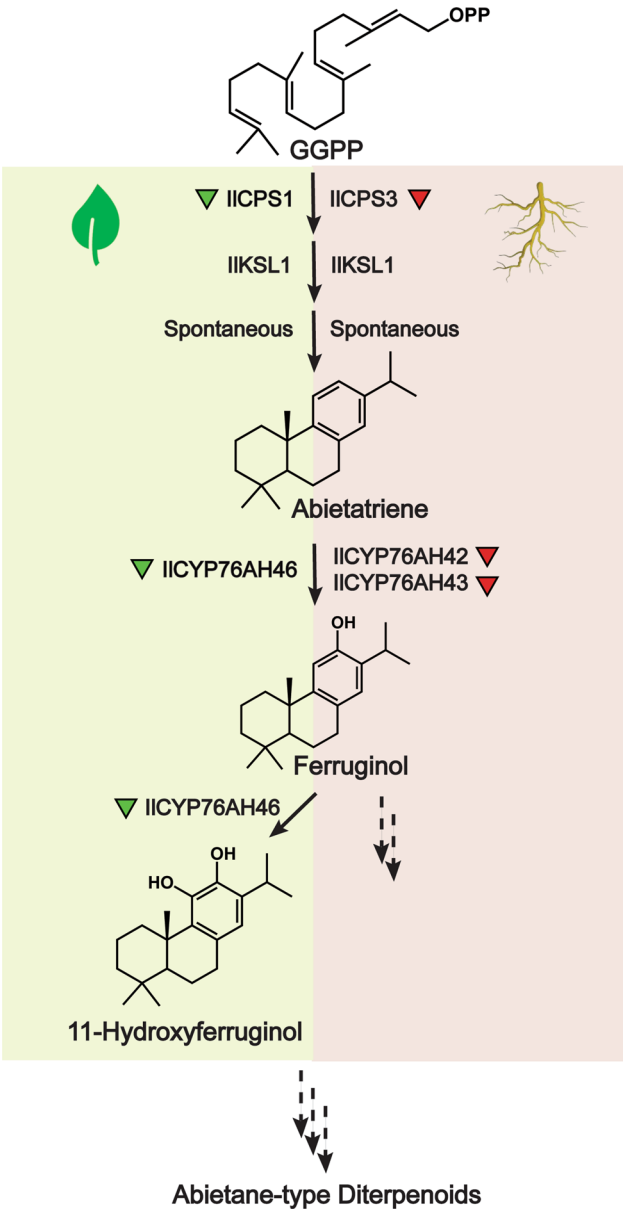

Fig. 6 Biosynthetic pathway of abietane diterpenoids in *I. lophanthoides*. Green and pink background indicates two independent biosynthetic pathways of ferruginol and 11-hydroxyferruginol in aerial and underground parts of *I. lophanthoides*. Dashed arrows indicate reactions without experimental evidences

to form ferruginol or 11-hydroxyferruginol. Despite their similar biochemical function, they share distinct expression patterns, protein sequence identities and genomic structures. Together with the previously identified (+)-CPSs, we proposed at least two independent biosynthetic pathways of abietane diterpenoids in the aerial and underground parts of *I. lophanthoides*. The root-preferential expressed CYP76AH42 and CYP76AH43 would account for the accumulation of ferruginol in the root periderms, while the product of CYP76AH46 in the aerial parts would likely undergo

further modification and form more complex abietanes. The physiological roles and evolution of these P450s need to be further explored.

Supplementary Information The online version contains supplementary material available at https://doi.org/10.1007/s00425-023-04125-z.

Acknowledgements Financial assistance was provided by the National Science Foundation of Distinguished Young Scholars of China (Grant No. 31900250).

Author contributions LH: designed the project; ZD, ZP, HY and HW: performed the experiments; JS: constructed the YS101 strain; LH: wrote the article. All the authors read and approved the manuscript.

Data availability The nucleotide sequences reported in this study have been deposited in the NCBI GenBankTM/EBI Data Bank with accession numbers: CYP76AH41, OP891584; CYP76AH42, OP891585; CYP76AH43, OP891586; CYP76AH44, OP891587; CYP76AH45, OP891588; CYP76AH46, OP891589; CYP76AH47, OP891590; CYP76AH48, OP891591; CYP76AH49, OP891592; CYP76AH50, OP891593; CYP76AH51, OP891594; CYP76AH52, OP891595.

Declarations

Conflict of interest The authors declare that they have no conflicts of interest.

References

Bathe U, Tissier A (2019a) Cytochrome P450 enzymes: a driving force of plant diterpene diversity. Phytochemistry 161:149–162. https://doi.org/10.1016/j.phytochem.2018.12.003

Bathe U, Frolov A, Porzel A, Tissier A (2019b) CYP76 oxidation network of abietane diterpenes in Lamiaceae reconstituted in Yeast. J Agric Food Chem 67:13437–13450. https://doi.org/10.1021/acs.jafc.9b00714

Božić D, Papaefthimiou D, Brückner K, de Vos RC, Tsoleridis CA, Katsarou D, Papanikolaou A, Pateraki I, Chatzopoulou FM, Dimitriadou E, Kostas S, Manzano D, Scheler U, Ferrer A, Tissier A, Makris AM, Kampranis SC, Kanellis AK (2015) Towards elucidating carnosic acid biosynthesis in Lamiaceae: functional characterization of the three first steps of the pathway in *Salvia fruticosa* and *Rosmarinus officinalis*. PLoS ONE 10:e0124106. https://doi.org/10.1371/journal.pone.0124106

Brandle JE, Telmer PG (2007) Steviol glycoside biosynthesis. Phytochemistry 68:1855–1863. https://doi.org/10.1016/j.phytochem.2007.02.010

Ceunen S, Geuns JM (2013) Steviol glycosides: chemical diversity, metabolism, and function. J Nat Prod 76:1201–1228. https://doi.org/10.1021/np400203b

Chen F, Tholl D, Bohlmann J, Pichersky E (2011) The family of terpene synthases in plants: a mid-size family of genes for specialized metabolism that is highly diversified throughout the kingdom. Plant J 66:212–229. https://doi.org/10.1111/j.1365-313X.2011.04520.x

Gietz RD, Woods RA (2002) Transformation of yeast by lithium acetate/single-stranded carrier DNA/polyethylene glycol method. Methods Enzymol 350:87–96. https://doi.org/10.1016/s0076-6879(02)50957-5

Guo J, Zhou YJ, Hillwig ML, Shen Y, Yang L, Wang Y, Zhang X, Liu W, Peters RJ, Chen X, Zhao ZK, Huang L (2013) CYP76AH1 catalyzes turnover of miltiradiene in tanshinones biosynthesis and enables heterologous production of ferruginol in yeasts. Proc Natl Acad Sci U S A 110:12108–12113. https://doi.org/10.1073/pnas.1218061110

Guo J, Ma X, Cai Y, Ma Y, Zhan Z, Zhou YJ, Liu W, Guan M, Yang J, Cui G, Kang L, Yang L, Shen Y, Tang J, Lin H, Ma X, Jin B, Liu Z, Peters RJ, Zhao ZK, Huang L (2016) Cytochrome P450 promiscuity leads to a bifurcating biosynthetic pathway for tanshinones. New Phytol 210:525–534. https://doi.org/10.1111/nph.13790

Hamberger B, Ohnishi T, Hamberger B, Séguin A, Bohlmann J (2011) Evolution of diterpene metabolism: Sitka spruce CYP720B4 catalyzes multiple oxidations in resin acid biosynthesis of conifer defense against insects. Plant Physiol 157:1677–1695. https://doi.org/10.1104/pp.111.185843

Hansen CC, Nelson DR, Møller BL, Werck-Reichhart D (2021) Plant cytochrome P450 plasticity and evolution. Mol Plant 14:1772. https://doi.org/10.1016/j.molp.2021.09.013

Hansen NL, Kjaerulff L, Heck QK, Forman V, Staerk D, Møller BL, Andersen-Ranberg J (2022) Tripterygium wilfordii cytochrome P450s catalyze the methyl shift and epoxidations in the biosynthesis of triptonide. Nat Commun 13:5011. https://doi.org/10.1038/s41467-022-32667-5

Ignea C, Athanasakoglou A, Ioannou E, Georgantea P, Trikka FA, Loupassaki S, Roussis V, Makris AM, Kampranis SC (2016) Carnosic acid biosynthesis elucidated by a synthetic biology platform. Proc Natl Acad Sci U S A 113:3681–3686. https://doi.org/10.1073/pnas.1523787113

Jin B, Cui G, Guo J, Tang J, Duan L, Lin H, Shen Y, Chen T, Zhang H, Huang L (2017) Functional diversification of kaurene synthase-like genes in *Isodon rubescens*. Plant Physiol 174:943–955. https://doi.org/10.1104/pp.17.00202

Ladeiras D, Monteiro CM, Pereira F, Reis CP, Afonso CA, Rijo P (2016) Reactivity of diterpenoid quinones: Royleanones. Curr Pharm Des 22:1682–1714. https://doi.org/10.2174/1381612822666151211094521

Lin L, Dong Y, Yang B, Zhao M (2011) Chemical constituents and biological activity of Chinese medicinal herb "Xihuangcao." Comb Chem High Throughput Screen 14:720–729. https://doi.org/10.2174/138620711796504352

Lin CZ, Zhao W, Feng XL, Liu FL, Zhu CC (2016) Cytotoxic diterpenoids from *Rabdosia lophanthoides* var. gerardianus. Fitoterapia 109:14–19. https://doi.org/10.1016/j.fitote.2015.11.015

Liu Q, Manzano D, Tanić N, Pesic M, Bankovic J, Pateraki I, Ricard L, Ferrer A, de Vos R, van de Krol S, Bouwmeester H (2014) Elucidation and in planta reconstitution of the parthenolide biosynthetic pathway. Metab Eng 23:145–153. https://doi.org/10.1016/j.ymben.2014.03.005

Liu M, Wang WG, Sun HD, Pu JX (2017) Diterpenoids from Isodon species: an update. Nat Prod Rep 34(9):1090–1140. https://doi.org/10.1039/c7np00027h

Ma Y, Cui G, Chen T, Ma X, Wang R, Jin B, Yang J, Kang L, Tang J, Lai C, Wang Y, Zhao Y, Shen Y, Zeng W, Peters RJ, Qi X, Guo J, Huang L (2021) Expansion within the CYP71D subfamily drives the heterocyclization of tanshinones synthesis in Salvia miltiorrhiza. Nat Commun 12:685. https://doi.org/10.1038/s41467-021-20959-1

Mafu S, Zerbe P (2017) Plant diterpenoid metabolis for manufacturing the biopharmaceuticals of tomorrow: prospects and challenges. Phytochem Rev 17:113–130. https://doi.org/10.1007/s11101-017-9513-5

Muchlinski A, Jia M, Tiedge K, Fell JS, Pelot KA, Chew L, Davisson D, Chen Y, Siegel J, Lovell JT, Zerbe P (2021) Cytochrome P450-catalyzed biosynthesis of furanoditerpenoids in the bioenergy crop switchgrass (*Panicum virgatum* L.). Plant J 108:1053–1068. https://doi.org/10.1111/tpj.15492

Pateraki I, Andersen-Ranberg J, Jensen NB, Wubshet SG, Heskes AM, Forman V, Hallström B, Hamberger B, Motawia MS, Olsen

CE, Staerk D, Hansen J, Møller BL, Hamberger B (2017) Total biosynthesis of the cyclic AMP booster forskolin from Coleus forskohlii. Elife 6:e23001. https://doi.org/10.7554/eLife.23001

Peng B, Plan MR, Carpenter A, Nielsen LK, Vickers CE (2017) Coupling gene regulatory patterns to bioprocess conditions to optimize synthetic metabolic modules for improved sesquiterpene production in yeast. Biotechnol Biofuels 10:43. https://doi.org/10.1186/s13068-017-0728-x

Ro DK, Arimura G, Lau SY, Piers E, Bohlmann J (2005) Loblolly pine abietadienol/abietadienal oxidase PtAO (CYP720B1) is a multifunctional, multisubstrate cytochrome P450 monooxygenase. Proc Natl Acad Sci U S A 102:8060–8065. https://doi.org/10.1073/pnas.0500825102

Sainsbury F, Thuenemann EC, Lomonossoff GP (2009) pEAQ: versatile expression vectors for easy and quick transient expression of heterologous proteins in plants. Plant Biotechnol J 7:682–693. https://doi.org/10.1111/j.1467-7652.2009.00434.x

Scheler U, Brandt W, Porzel A, Rothe K, Manzano D, Božić D, Papaefthimiou D, Balcke GU, Henning A, Lohse S, Marillonnet S, Kanellis AK, Ferrer A, Tissier A (2016) Elucidation of the biosynthesis of carnosic acid and its reconstitution in yeast. Nat Commun 7:12942. https://doi.org/10.1038/ncomms12942

Sun HD, Huang SX, Han QB (2006) Diterpenoids from Isodon species and their biological activities. Nat Prod Rep 23:673–698. https://doi.org/10.1039/b604174d

Tamura K, Stecher G, Kumar S (2021) MEGA11: molecular evolutionary genetics analysis version 11. Mol Biol Evol 38:3022–3027. https://doi.org/10.1093/molbev/msab120

Ting HM, Wang B, Rydén AM, Woittiez L, van Herpen T, Verstappen FWA, Ruyter-Spira C, Beekwilder J, Bouwmeester HJ, van der Krol A (2013) The metabolite chemotype of *Nicotiana benthamiana* transiently expressing artemisinin biosynthetic pathway genes is a function of CYP71AV1 type and relative gene dosage. New Phytol 199:352–366. https://doi.org/10.1111/nph.12274

Tu L, Su P, Zhang Z, Gao L, Wang J, Hu T, Zhou J, Zhang Y, Zhao Y, Liu Y, Song Y, Tong Y, Lu Y, Yang J, Xu C, Jia M, Peters RJ, Huang L, Gao W (2020) Genome of Tripterygium wilfordii and identification of cytochrome P450 involved in triptolide biosynthesis. Nat Commun 11:971. https://doi.org/10.1038/s41467-020-14776-1

van Herpen TW, Cankar K, Nogueira M, Bosch D, Bouwmeester HJ, Beekwilder J (2010) Nicotiana benthamiana as a production platform for artemisinin precursors. PLoS ONE 5:e14222. https://doi.org/10.1371/journal.pone.0014222

Wang Q, Hillwig ML, Okada K, Yamazaki K, Wu Y, Swaminathan S, Yamane H, Peters RJ (2012) Characterization of CYP76M5-8 indicates metabolic plasticity within a plant biosynthetic gene cluster. J Biol Chem 287:6159–6168. https://doi.org/10.1074/jbc.M111.305599

Wu Y, Hillwig ML, Wang Q, Peters RJ (2011) Parsing a multifunctional biosynthetic gene cluster from rice: biochemical characterization of CYP71Z6&7. FEBS Lett 585:3446–3451. https://doi.org/10.1016/j.febslet.2011.09.038

Wu Y, Wang Q, Hillwig ML, Peters RJ (2013) Picking sides: distinct roles for CYP76M6 and CYP76M8 in rice oryzalexin biosynthesis. Biochem J 454:209–216. https://doi.org/10.1042/BJ20130574

Xiong X, Gou J, Liao Q, Li Y, Zhou Q, Bi G, Li C, Du R, Wang X, Sun T, Guo L, Liang H, Lu P, Wu Y, Zhang Z, Ro DK, Shang Y, Huang S, Yan J (2021) The Taxus genome provides insights into paclitaxel biosynthesis. Nat Plants 7:1026–1036. https://doi.org/10.1038/s41477-021-00963-5

Yang LB, Li L, Huang SX, Pu JX, Zhao Y, Ma YB, Chen JJ, Leng CH, Tao ZM, Sun HD (2011) Anti-hepatitis B virus and cytotoxic diterpenoids from *Isodon lophanthoides* var. gerardianus. Chem Pharm Bull 59:1102–1105. https://doi.org/10.1248/cpb.59.1102

Yang R, Du Z, Qiu T, Sun J, Shen Y, Huang L (2021) Discovery and functional characterization of a diverse diterpene synthase family in the medicinal herb *Isodon lophanthoides* Var. gerardiana. Plant Cell Physiol 62:1423–1435. https://doi.org/10.1093/pcp/pcab089

Zi J, Peters RJ (2013) Characterization of CYP76AH4 clarifies phenolic diterpenoid biosynthesis in the Lamiaceae. Org Biomol Chem 11:7650–7652. https://doi.org/10.1039/c3ob41885e

Zi J, Mafu S, Peters RJ (2014) To gibberellins and beyond! Surveying the evolution of (di)terpenoid metabolism. Annu Rev Plant Biol 65:259–286. https://doi.org/10.1146/annurev-arplant-050213-035705